(20) Freche, P.; Grenier-Loustalot, M. F. *J. Polym. Sci., Polym. Chem. Ed.* **1983**, *21*, 2755.
(21) Freche, P.; Grenier-Loustalot, M. F.; Metras, F. *Makromol. Chem.* **1983**, *184*, 5691.
(22) Roedel, M. J. *J. Am. Chem. Soc.* **1953**, *75*, 6110.
(23) Willbourn, A. H. *J. Polym. Sci.* **1959**, *34*, 569.
(24) Foster, G.; MacRury, T.; Hamielec, A. In "Liquid Chromatography of Polymers and Related Materials"; Marcel Dekker: New York, 1980; Vol. 13, p 143.
(25) Hert, M.; Strazielle, C. *Makromol. Chem.* **1983**, *184*, 135.
(26) Rault, J. *J. Phys., Lett. (Orsay, Fr.)* **1978**, *39*, L411.
(27) Candau, F.; Rempp, P.; Benoit, H. *Macromolecules* **1972**, *5*, 627. Candau, F.; Strazielle, C.; Benoit, H. *Makromol. Chem.* **1972**, *165*, 1.
(28) Thurmond, C.; Zimm, B. *J. Polym. Sci.* **1952**, *8*, 477.
(29) Nagasubramanian, K.; Saito, O.; Graessley, W. *J. Polym. Sci., Part A-2* **1969**, *7*, 1955.
(30) Bohdanecký, M. *Macromolecules* **1977**, *10* (5), 971.
(31) Yamakawa, H. "Modern Theory of Polymer Solutions"; Wiley: New York, 1971.

Structure of Peroxy Radicals Trapped in Irradiated Isotactic Polypropylene and Molecular Disorder of the Polymer Chain, Related with Hydrogen Abstraction Reaction of the Radicals

Shigetaka Shimada, Yasurō Hori, and Hisatsugu Kashiwabara*

Nagoya Institute of Technology, Gokiso-cho, Showa-ku, Nagoya 466, Japan.
Received June 11, 1984

ABSTRACT: The conformational structure of peroxy radicals and the molecular disorder of a polymer chain in elongated isotactic polypropylene with a stretch ratio of 6 are determined from the angular dependences of the ESR spectra, which can be simulated from the calculated spectra of the partially oriented paramagnetic centers. The internal rotation angle which represents the orientation of the O–O group around the C–O bond with respect to the adjacent C–C bond, $\phi_m = -103° \pm 5°$, and the degree of orientation, $f_m = 0.536$, are estimated for mobile peroxy radicals, which decay substantially at room temperature. In addition, the internal rotation angle, $\phi_r = 55.5° \pm 1.5°$, and the degree of orientation, $f_r = 0.968$, are determined for rigid peroxy radicals, which are very stable at room temperature. The values of $\phi_m = -103°$ and $\phi_r = 55.5°$ are close to −120° and 60°, corresponding to skew and gauche conformations, respectively. The high degree of orientation, $f_r = 0.968$, is in good agreement with that of the polymer chain in crystalline regions, 0.93, obtained by X-ray diffraction. It is concluded that the mobile peroxy radicals are trapped at disordered sites in the crystalline regions, although the rigid peroxy radicals are at highly ordered sites in the same region. The reactivity of the interchain hydrogen abstraction of the mobile peroxy radicals is discussed in comparison with the rigid peroxy radicals on the basis of their conformational structures and the molecular orientations.

Introduction

Spin-label and spin-probe techniques have been developed to study the structure and dynamic behavior of polymer chains at a particular site or a particular region. We have undertaken ESR studies of much smaller spin labels, for example, alkyl radicals and peroxy radicals[1] bonded to the polymer chain. The small labels are more desirable for the study of the polymer properties than the large spin labels commonly used.

In this report, the conformational structure of peroxy radicals in isotactic polypropylene and the molecular disorder of the polymer chain are discussed on the basis of the angular dependences of the ESR spectra.

One of the purposes of the present study is to contribute to the investigation of the reaction mechanism of peroxy radicals. Eda et al.[2] and Hori et al.[3] found that the ESR spectra of peroxy radicals trapped in irradiated isotactic polypropylene are composed of two spectra arising from chemically identical peroxy radicals having different mobilities. Hori et al.[3] recently suggested very interesting conclusions: (1) The mobile peroxy radicals are trapped in crystalline regions and decay by a diffusion controlled mechanism. (2) The main mechanism is the intermolecular hydrogen abstraction by the peroxy radicals. (3) The rigid peroxy radicals are stable and the quantity of the radicals decreases with reaction temperature.

We raise two questions: Why are the mobilities of the two kinds of peroxy radicals trapped in the crystalline sites different and why do the mobile peroxy radicals abstract hydrogen intermolecularly.[3] In order to answer these questions, one must acquire a knowledge of the surrounding conditions of the peroxy radicals, for instance, the molecular orientations of the polymer chain and the conformational structures of the radicals.

Another purpose in the present article is to find a simple method for the determination of orientations in polymer materials composed of more than two different regions, the amorphous, pseudocrystalline, and crystalline, by a spin-label technique. These orientations have generally been determined by X-ray diffraction, birefringence, and sonic absorption measurements and combining them. For example, we can estimate the orientation in the region with a knowledge of the sample crystallinity and the corresponding orientation function for the crystalline region.[4] However, a shortcoming of the indirect method is that the estimated value may be subject to cumulative errors. The direct spin-label method may offer some distinct advantages for the study of local molecular orientations in the polymer sample, such as the orientations of the amorphous and crystalline regions, the interior and terminal portions of the polymer chains and the molecularly disordered regions, by introducing spin labels into these regions. An ESR method for the determination of orientations in the amorphous region by using $C_2F_4^-$ radicals has been published.[5]

In this paper, we compare the degree of orientation of the peroxy radicals in the crystalline region with that of polymer chains in the same region, obtained by X-ray diffraction measurement, and show that the ESR method is simple and effective for the determination of the ori-

0024-9297/85/2218-0170$01.50/0

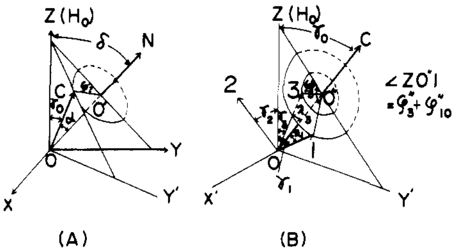

Figure 1. Geometrical relationship for a main chain axis (OC) in a laboratory axis system (OX, OY, OZ) (A) and a principal axis system (O1, O2, O3) of the **g** tensor (B). An external field (OZ) and a stretching direction are represented in the plane, YZ.

entation of the polymer chains.

Experimental Section

An isotactic polypropylene, Noblen MA-4 (product of Mitsubishi Petrochemical Co. Ltd., $\bar{M}_v = 40 \times 10^4$) was used for this study. The sample was purified three times by dissolving it in boiling toluene, precipitating it by cooling, and washing it in acetone. After drying in a vacuum oven, the powdered sample was heated to 473 K and pressed into a film which was subsequently stretched at 393 K to a stretch ratio of 6. This elongated film (ca. 1 mm thick) was then cut into narrow strips which were placed in a Spectrosil sample tube. This sample was prepared with the stretching direction perpendicular to the axis of the sample tube. The sample was evacuated to 10^{-5} torr and then irradiated at ambient temperature with ^{60}Co γ-ray to a total dose of ca. 4.25 Mrad. After it was verified that only the tertiary alkyl radicals of polypropylene ($\sim CH_2\text{-}\dot{C}(Me)\text{-}CH_2\sim$) were trapped by observing the 17-line ESR spectrum at room temperature, oxygen at a pressure of 200 torr was introduced into the sample tube.

The ESR measurements were carried out with a JEOL ME-3X X-band spectrometer with 100-kHz modulation. The spectra were recorded with a MELCOM 70/25 computer connected to the spectrometer. The signal of diphenylpicrylhydrazyl (DPPH) was used as a g-value standard. The magnetic field sweep was calibrated with known splitting constants of Mn^{2+}. X-ray diffraction was carried out with a RAD-IIA (Rigaku Denki Co.) diffractometer in order to estimate the c-axis orientation function of the polypropylene crystal, $f_\alpha = \langle(3 \cos^2 \alpha - 1)/2\rangle$, where α is the angle between a stretching direction (N) and the c axis. The value of f_α was similarly evaluated in terms of the orientation of plane normals, expressed as $\langle(3 \cos^2 \phi - 1)/2\rangle$, where ϕ is the angle between N and the normal to a set of hkl planes.[6,7] In this article, the azimuthal intensity distributions $I(\phi)$, of the (040) and (110) planes were obtained from the intensity distributions of the X-ray diffraction at the Bragg angle for the angles, ϕ, after it was confirmed that molecular orientation around the N axis was isotropic.

By the established method,[8] the X-ray diffraction patterns with the increment angle, $\Delta\phi$, of 5° were found to be composed of (040), (110), (130), and amorphous reflections, and the exact intensities of $I(\phi)$ for (040) and (110) planes were evaluated. Then, the value of f_α was calculated from the following equation:[6,7]

$$f_\alpha = -0.901\left(\frac{3\langle\cos^2 \phi\rangle_{040} - 1}{2}\right) - 1.099\left(\frac{3\langle\cos^2 \phi\rangle_{110} - 1}{2}\right)$$

Simulation

In order to obtain the ESR spectra of partially and uniaxially oriented peroxy radicals, one must calculate the resonance magnetic field, $H_r(\Omega)$ and the intensity of the ESR transition, $I(H_r)$ for a peroxy radical with a particular arbitrary orientation with respect to an external field. Ω represents the set of direction cosines of the external field, ($\cos \gamma_1$, $\cos \gamma_2$, $\cos \gamma_3$), expressed in the principal axis system. Figure 1A represents the geometrical relationship for the main chain axis (OC) in a laboratory system. The Z axis is the direction of the external field (OZ) and the stretching direction (ON) is represented in the plane, YZ. The angle γ_0 between OZ and OC can be obtained from

$$\cos \gamma_0 = \cos \delta \cos \alpha + \sin \delta \sin \alpha \cos \phi' \qquad (1)$$

where δ is an experimental rotation angle between OZ and ON and α is the distribution angle between ON and OC. The angle ϕ' can be defined as the dihedral angle between the planes OZO′ and OCO′. The uniaxial orientation of cylindrical symmetry around the stretching direction means that the distribution of the chain axis has an equal probability around the direction (ON). Then, the observed spectrum can be simulated by integrating over all possible orientations with appropriate weighting for the angle α and equal weighting for the angle ϕ'.

The principal directions of the magnetic tensor can be added in the system, X′Y′Z as represented in Figure 1B. λ_1, λ_2, and λ_3 can be defined as the angles between the principal directions of the **g** tensor, O1, O2, and O3, and the polymer chain axis, OC, respectively. In order to calculate the value of $H_r(\Omega)$, the angle Ω can be obtained from the following equations:

$$\cos \gamma_3 = \cos \gamma_0 \cos \lambda_3 + \sin \gamma_0 \sin \lambda_3 \cos \phi_3'' \qquad (2)$$

$$\cos \gamma_1 = \cos \gamma_0 \cos \lambda_1 + \sin \gamma_0 \sin \lambda_1 \cos (\phi_3'' + \phi_{10}'') \qquad (3)$$

$$\cos \phi_{10}'' = (-\cos \lambda_3 \cos \lambda_1)/(\sin \lambda_3 \sin \lambda_1) \qquad (4)$$

$$\cos \gamma_2 = \pm(1 - \cos^2 \gamma_1 - \cos^2 \gamma_2)^{1/2} \qquad (5)$$

$$H_r(\Omega) = h\nu/g(\Omega)\beta \qquad (6)$$

$$g^2(\Omega) = g_1^2 \cos^2 \gamma_1 + g_2^2 \cos^2 \gamma_2 + g_3^2 \cos^2 \gamma_3 \qquad (7)$$

where $h\nu$ and β represent the microwave energy and the Bohr magneton, respectively, and g_1, g_2, and g_3 are the principal values of the **g** tensor. The angle ϕ_3'' means the dihedral angle between the planes, OZO″ and O3O″ as shown in Figure 1B. The intensity, $I(H_r)$ is proportional to the number of peroxy radicals, for instance, the distribution function $P(\alpha)$. $P(\alpha)$ is assumed to be a Gaussian distribution, $\exp(a \sin^2 \alpha)$.[9] For the determination of the orientation function f_α and the angles, λ_1, λ_2, and λ_3, the computer simulation was made in the following procedure.

(a) The distribution function, $P(\alpha)$ is calculated for all angles of α using a given parameter of a and the results are stored in the computer.

(b) For the arbitrary angle of rotation, δ, the direction cosines of $\cos \gamma_1$, $\cos \gamma_2$, and $\cos \gamma_3$ are calculated for all sets of α, ϕ', and ϕ_3'', using given parameters λ_1 and λ_3 (eq 1–5).

(c) The resonance field $H_r(\Omega)$ is calculated by using the principal values, $g_1 = 2.0021$, $g_2 = 2.0081$, and $g_3 = 2.0353$, which are obtained from the simulation of the powdered sample[10] (eq 6–7).

(d) The final ESR spectrum, $I(H)$, can be calculated from the convolution of $P(\alpha)$ and line shape function G as follows:

$$I(H) = \int_0^{2\pi} \int_0^{\pi} \int_0^{\pi/2} P(\alpha) G\{(H - H_r(\Omega)), \mathrm{Dh}\}\, d\alpha\, d\phi'\, d\phi_3'' \qquad (8)$$

The line width, Dh, which was determined from the simulation of the powdered sample, was also used in eq 8.

Several theoretical spectra were calculated by changing the values of a, λ_1, and λ_3 gradually. These spectra were recorded on an X-Y plotter and compared with the observed spectra in order to get the best fit. From the determined values of λ_1 and λ_3, the structure of the peroxy radical can be discussed in the next section and from the

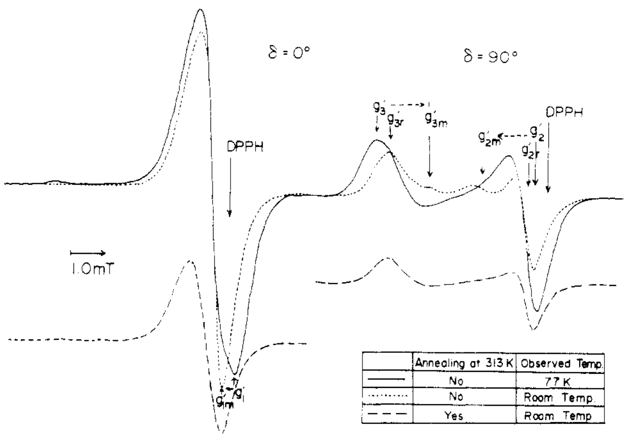

Figure 2. Examples of angular dependent ESR spectra of peroxy radicals trapped in the stretched *it*-polypropylene film. The angle δ means the angle between the direction of elongation and that of the external magnetic field. Other experimental conditions are represented in the figure.

value determined for a, the orientation function f_α is calculated as follows:

$$f_\alpha = \frac{\int_0^{\pi/2} \{(3\cos^2\alpha - 1)/2\} \exp(a \sin^2\alpha)\, d\alpha}{\int_0^{\pi/2} \exp(a \sin^2\alpha)\, d\alpha}$$

Results and Discussion

1. ESR Spectra of Peroxy Radicals in Irradiated *it*-Polypropylene. The peroxy radicals were produced by reaction of the alkyl radicals with oxygen at 263 K for 33 h. Figure 2 shows examples of ESR spectra of peroxy radicals trapped in the stretched *it*-polypropylene film after annealing at room temperature for 85 h. A very marked angular dependence of the ESR spectra suggests a preferential orientation of the polymer main chain along the stretching direction. On the other hand, no angular dependence of the ESR spectra with respect to the external magnetic field was observed when the sample was prepared with the stretching direction parallel to the axis of the sample tube. This demonstrates that the main chain axis has a uniaxially preferential orientation of cylindrical symmetry around the stretching direction. As shown in Figure 2, it was found that the ESR spectra are composed of two spectra arising from chemically identical peroxy radicals having different mobilities and stabilities. The arrows in Figure 2 indicate the representative resonance fields, g_1', g_2', and g_3', which can be considered to be an approximate standard for the g values, parallel (g_1') and perpendicular (g_2' and g_3') to the stretching direction. The mobile peroxy radicals $(\mathrm{ROO}\cdot)_\mathrm{m}$ decayed under annealing at 313 K whereas the rigid peroxy radicals $(\mathrm{ROO}\cdot)_\mathrm{r}$ are more stable. For example, the representative resonance field, $g_{2\mathrm{m}}'$ and $g_{3\mathrm{m}}'$, attributed to the mobile peroxy radicals disappeared under annealing. The value of $g_{2\mathrm{m}}'$ and $g_{3\mathrm{m}}'$ showed a remarkable shift in comparison with the $g_{1\mathrm{m}}'$ values with increasing observation temperature.

The values of $g_{2\mathrm{m}}'$ and $g_{3\mathrm{m}}'$ for the mobile peroxy radicals correspond to the g values perpendicular to the main chain, whereas the value of $g_{1\mathrm{m}}'$ corresponds to the g value parallel to the chain. These facts suggest that the motion of the mobile and less stable peroxy radicals is a rotation or a rotatory vibration of the COO group around the polymer main chain. These results are consistent with the conclusion in previous papers.[10]

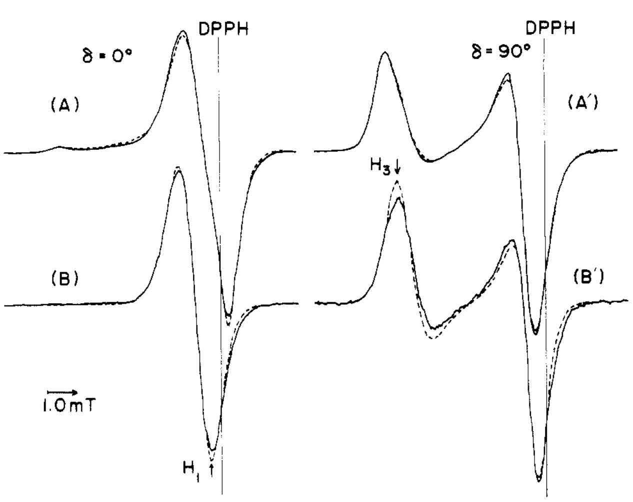

Figure 3. Variation of the observed (solid) and calculated (dotted) ESR spectra of peroxy radicals trapped in isotactic polypropylene before ((A), (A′)) and after ((B), (B′)) heat treatment at 313 K for 40 h. The meaning of δ is represented in Figure 2. ESR spectra were observed at 77 K. No significance should be attached to the relative intensity of these four spectra. The calculated spectra (A) and (A′) are composed of two spectra of rigid radicals ((B) and (B′) in Figure 3, 22–26%) and mobile radicals (Figure 7, 74–78%). The calculated spectra (B) and (B′) were obtained by using the values of $\lambda_1 = 39°$, $\lambda_3 = 68°$, and $f = 0.968$.

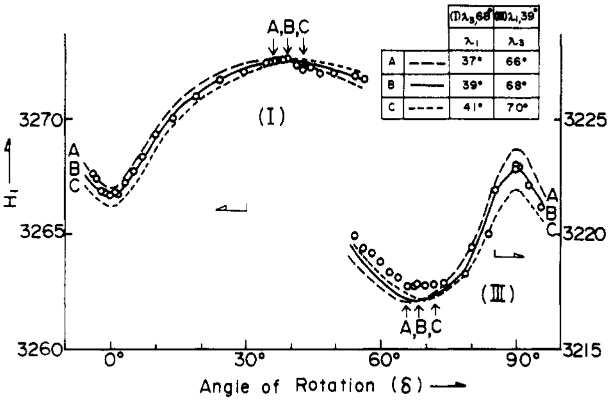

Figure 4. Angular dependences of the characteristic resonance field of the rigid peroxy radicals trapped in isotactic polypropylene upon rotation angles (δ). The open circles indicate observed values at 77 K. The lines are calculated for the parameters of λ_1 and λ_3, represented in the figure and $f = 0.968$.

2. Structure of Rigid Radical and Molecular Orientation of the Polymer Chain. Figure 3B shows the ESR spectra of rigid peroxy radicals trapped in crystalline regions after the sample was annealed at 313 K for 40 h. The ESR spectrum showed a very marked angular dependence with the external magnetic field along the stretching direction ($\delta = 0°$), the intensity of the g_1 feature is enhanced. On the other hand, the ESR spectrum shows g_2 and g_3 features for the field perpendicular to the stretching direction ($\delta = 90°$). However, the g value corresponding to the characteristic resonance field, 2.0051 for $\delta = 0°$ is different from $g_1 = 2.0021$ obtained previously from the ESR spectrum of an unoriented sample (the directions of g_1, g_2, and g_3 are represented in Figure 6).

Figure 4 shows the angular dependence of the characteristic resonance field, H_1 and H_3, which are indicated in Figure 3. We can observe very strong dependences of the values of H_1 and H_3 on the rotation angle H_1 for $\delta = 39°$ giving a maximum value and H_3 for $\delta = 68°$ giving a minimum value. The g values corresponding to the maximum and minimum resonance field are in good agreement with the principal values of the peroxy radicals of *it*-PP, $g_1 = 2.0021$ and $g_3 = 2.0353$, respectively. The angles between the principal directions of the **g** tensor and the

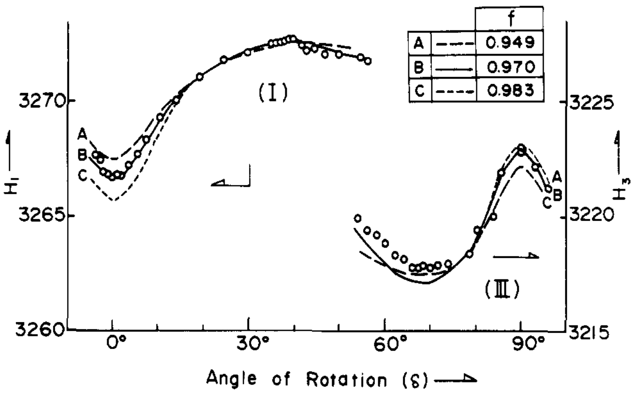

Figure 5. Angular dependences of the characteristic resonance field of the rigid peroxy radicals trapped in isotactic polypropylene upon rotation angles (δ). The open circles indicate observed values at 77 K. The lines are calculated for the parameter of f, represented in the figure and $\lambda_1 = 39°$ and $\lambda_3 = 68°$.

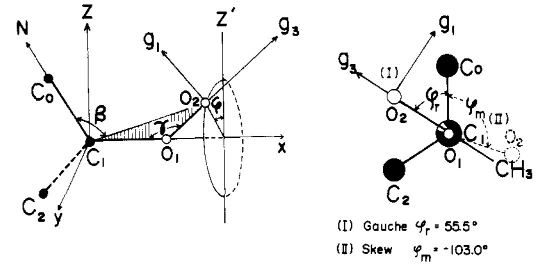

Figure 6. Schematic illustration of peroxy radical of isotactic polypropylene. The polymer main chain axis are taken to be parallel to direction of C_0–C_1 bond in 3_1 helical structure of *it*-PP crystal. The angle ϕ is the internal rotation angle. ϕ_r and ϕ_m are the angles corresponding to the rigid and mobile peroxy radicals, respectively, as interpreted in the text. g_1; perpendicular to the COO plane, g_3; the direction of the O–O bond, g_2; perpendicular to g_1 and g_3.

polymer main chain axis can be estimated to be $\lambda_{1r} = 39°$ and $\lambda_{3r} = 68°$. In order to estimate the angles exactly, a computer simulation mentioned above was performed. Computer-simulated spectra were generated for different orientation parameters f and angles, λ_1 and λ_3, and the characteristic fields, H_1 and H_3, estimated from the simulated spectra were plotted as shown in Figures 4 and 5. As expected, the simulated spectra have very strong dependences on the degree of order f and these angles. The profiles of the experimental spectra (solid lines) show good agreement with the spectra calculated (dotted lines) in Figure 3 for $f_r = 0.968$, $\lambda_{1r} = 39°$, and $\lambda_{3r} = 68°$. The angular dependences of the experimental resonance field also show good agreements with those of the calculated field for the same values of f_r, λ_{1r}, and λ_{3r} as shown in Figures 4 and 5. By the computer simulation method, we determined the values of f_r, λ_{1r}, and λ_{3r} to be 0.968 ± 0.010, 39° ± 1°, and 68° ± 1°, respectively.

On the basis of the estimated values of λ_1 and λ_3, one can then determine the structure of the rigid peroxy radical. Figure 6 represents the orientation of the O–O group around the C–O bond with respect to the adjacent C_0–C_1 bond. The angle ϕ is the internal rotation angle. It can safely be assumed that the 3_1 helical structure remains unchanged and that the direction of C_0–C_1 is parallel to the main chain axis when a peroxy radical is formed. Therefore, the direction cosines of C_1N, g_1, and g_3 with respect to X, Y, and Z axes in Figure 6 can be obtained as follows:

$$C_1N(\cos\beta,\ 0,\ \sin\beta),\ g_1(0,\ -\cos\phi,\ \sin\phi)$$

$$g_3(-\cos\gamma,\ \sin\gamma\sin\phi,\ \sin\gamma\cos\phi) \tag{8}$$

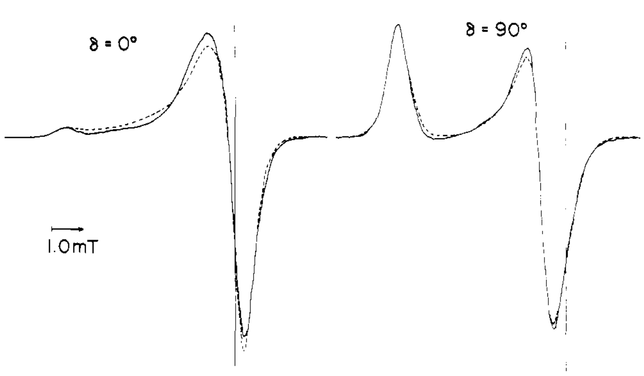

Figure 7. Angular-dependent ESR spectra of mobile peroxy radicals obtained by subtracting a considerable amount of the ESR spectra after annealing (Figure 3B) from those before annealing (Figure 3A). The calculated spectra were obtained by using $\lambda_1 = 24°$, $\lambda_3 = 73°$ and $f = 0.536$.

where β and γ mean the bond angles $\angle C_0C_1O_1$ and $\angle C_1O_1O_2$, respectively. Then, the angles of λ_1 and λ_3 can be obtained from the following equations:

$$\cos\lambda_1 = \sin\beta\sin\phi \tag{9}$$

$$\cos\lambda_3 = -\cos\beta\cos\gamma + \sin\beta\sin\gamma\cos\phi \tag{10}$$

Equations 9 and 10 lead to

$$\cos\gamma = -\cos\lambda_1\cos\beta - \frac{[(1 - \cos^2\lambda_1 - \cos^2\beta)(1 - \cos^2\lambda_1 - \cos^2\lambda_3)]^{1/2}}{(1 - \cos^2\lambda_1)} \tag{11}$$

$\gamma = 111°{}_{-1°}^{+2°}$ and $\phi_r = 55.5° \pm 1.5°$ can be obtained from eq 9 and 10 when the angle, $\beta = 109°28'$ (tetrahedral angle) and the observed angles, $\lambda_{1r} = 39° \pm 1°$ and $\lambda_{3r} = 68° \pm 1°$. The value of ϕ_r, 55.5°, is close to 60°, corresponding to the gauche conformation. The molecular disorder of the polymer chain and the trapped region of the rigid peroxy radicals can next be discussed. The degree of order $f_r = 0.968$ was very close to 0.930, corresponding to the orientation function of the main chain axis (c axis) of *it*-PP crystals estimated by the X-ray diffraction method. From this fact it can be concluded that the rigid peroxy radicals are trapped in the crystalline ordered region and the ESR spectrum for the radicals are effective for the determination of the orientation function in the crystalline region.

3. Structure of Mobile Peroxy Radicals and Molecular Disorder of the Polymer Chain. The angular dependence of the ESR spectra of the rigid peroxy radicals was completely analyzed using the three parameters f, λ_1, and λ_3 in the previous section. In order to elucidate the structure and molecular disorder of the mobile peroxy radicals, the ESR spectra must be analyzed by the same method. Figure 7 shows the ESR spectra of the mobile peroxy radicals obtained by subtraction of the considerable contribution of the rigid peroxy radicals, the ESR spectra of which are shown in Figure 3B from the observed ESR spectra before annealing (Figure 3A). The subtraction of 22–26% of the rigid peroxy radicals from the whole radical concentration before annealing gave the smoothed ESR spectra of the mobile peroxy radicals. For example, it was found that the ESR spectra before annealing arise from the rigid peroxy radicals to the extent of 22–26% and from the mobile ones to the extent of 74–78%. As expected, computer simulated spectra for the mobile peroxy radicals also have a very strong dependence on the degree of order f and tne angles, λ_1 and λ_3. The profiles of the epxerimental spectra (solid line) show good agreement with the spectra calculated (dotted line) in Figure 7 for $f_m = 0.536$,

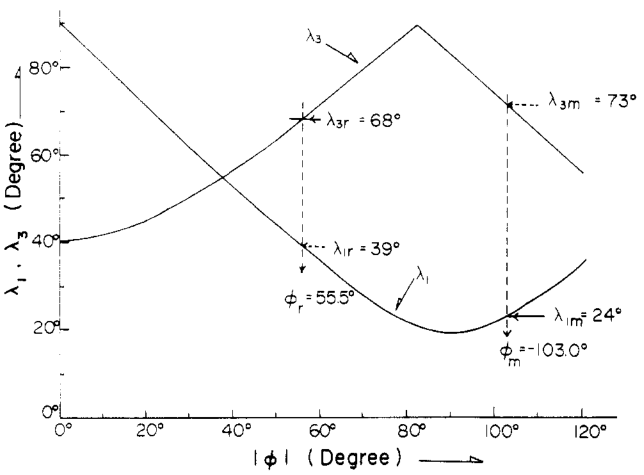

Figure 8. Relation between the angle λ and the internal rotation angle, ϕ, obtained from eq 9 and 10.

$\lambda_1 = 24°$, and $\lambda_3 = 73°$. The smaller value of $f_m = 0.536$ compared to $f_r = 0.968$ for the rigid peroxy radicals suggests that the mobile peroxy radicals are trapped in the disordered region in contrast to the rigid peroxy radicals. The trapped sites of the radicals will be discussed in detail in the next section. The relation between the angle λ and the internal rotation angle, ϕ, can be represented in Figure 8 by using eq 11 with the values $\beta = 109°28'$ and $\gamma = 111°$. The angle $\phi_m = -103° \pm 5°$ for the mobile peroxy radicals can be estimated for the values of $\lambda_{1m} = 24° \pm 2°$ and $\lambda_{3m} = 73° \pm 2°$ from Figure 8. The value of $\phi_m = -103°$ is fairly close to $-120°$ corresponding to the skew conformation, as represented in Figure 6. Iwasaki et al.[11] and Hori et al.[1c,12] concluded that the COO group lies in the plane perpendicular to the polymer main chain axis, the polymer chain having a planar zigzag conformation like that of polyethylene or a slightly distorted planar zigzag structure like that of poly(tetrafluoroethylene). This conclusion suggests the orientation of the O–O bond is gauche ($\phi = 60°$) or skew ($\phi = -120°$) to the adjacent C–C bond. If the conformation of the peroxy radicals is not strongly affected by the structure of the main chain, $\phi_r = -55.5°$ and $\phi_m = 103.0°$ in the case of *it*-PP should be dismissed. The values of $-55.5°$ and $103.0°$ obtained from eq 11 are inconsistent with $\phi = 60°$ or $-120°$ in the cases of PE and PTFE. Therefore, the values of $\phi_r = 55.5°$ and $\phi_m = -103.0°$ mentioned above were adopted. The deviations of 4.5° and 17° from the gauche and skew conformations, respectively, may be caused by the fact that the 3_1 helical structure deviates very much from a planar zigzag conformation. It is very interesting that two chemically identical peroxy radicals having different mobilities have different conformations and extents of molecular disorder.

4. Location and Trapping Site of Mobile Peroxy Radicals. In the previous section, it was concluded that the rigid peroxy radicals should be trapped in the crystalline ordered region. The next question whether the location of the mobile peroxy radicals is the inner crystalline or the amorphous region, including the crystalline surface. The peroxy radicals observed in this study were produced by oxygenation of stable tertiary alkyl radicals remaining at 313 K, higher than the glass–rubber transition temperature, 260 K, for 2 h.

This suggests that the alkyl radicals are trapped in the inner crystalline region. Kusumoto et al.[13] concluded from the ESR nonette resonance that radicals corresponding to the alkyl radicals are trapped in the lamellar crystal, presumably in crystalline defects produced by means of nitric acid etching of various polypropylene sample. On the other hand, Fisher et al.[14] found the hydrogen abstraction of peroxy radicals and Eda et al.[2] demonstrated that migration of radicals or a change of the surrounding matrix itself occured during the production of mobile peroxy radicals and hydrogen abstraction. Eda et al. also concluded that the alkyl radicals (they called them carbon radicals) produced by the hydrogen abstraction reaction of the mobile peroxy radicals contribute to the graft reaction with styrene monomer trapped in the amorphous region.[15] These facts suggest two possibilities about the trapping region of the mobile peroxy radicals.

Case (A): The mobile peroxy radicals are trapped in the amorphous region and both reactions (I) and (II)

$$\text{the carbon radicals} \underset{\text{(II) in vacuum}}{\overset{\text{(I) } O_2}{\rightleftarrows}} \text{the mobile peroxy radicals}$$

should be mainly in the same region.

Case (B): The mobile peroxy radicals are trapped in the crystalline region and both reactions (I) and (II) should be mainly in the same region. In both (A) and (B), the migration of the carbon radicals from the inner crystalline to the amorphous part or from the amorphous to the inner crystalline occurred. Graft copolymerization[15] can be interpreted in terms of migration reactions from the inner crystalline to the amorphous.

In order to elucidate the nature of trapping region of the mobile peroxy radicals, case (A) or case (B), one must estimate the reaction rate of the oxygenation (I) in comparison with that of the migration of the carbon radicals. The trapping region of the carbon radicals is the inner crystalline as clarified by Kusumoto et al.[13] Therefore, case (B) applies when oxygen molecules can diffuse rapidly into the inner crystalline in comparison with the migration rate of the carbon radicals. On the other hand, if the diffusion of oxygen molecules in the crystalline regions is very slow, but that in the amorphous region is very fast, the rate of the oxygenation is controlled by the rate of the migration of the carbon radicals and case (A) applies.

It was found that the carbon radicals are very stable under vacuum at room temperature, but the conversion of the carbon radicals to the mobile peroxy radicals is complete in less than 1 h at the same temperature. These facts suggest that the mobile peroxy radicals should be trapped in the inner crystalline region; therefore, case (B) applies. It can be considered that the very slow migration of the carbon radicals to the amorphous region contributes to graft[15] copolymerization in the same region. It can also be reasonably concluded that large numbers of mobile peroxy radicals (74–78%) are located in the molecularly disordered sites of the inner crystalline in *it*-polypropylene samples with high crystallinity. The low orientation function, $f_m = 0.536$, points to molecularly disordered sites such as defects in the crystals, including conformational distortion, caused by the bonding of oxygen molecules. The difference between the mobility of the mobile peroxy radical and that of the rigid radical can be considered to come from their molecular disorder. This conclusion concerning the location of the mobile peroxy radicals is consistent with the conclusion from the mechanism of the decay reaction by Hori et al.[3]

5. Intermolecular Hydrogen Abstraction of Mobile Peroxy Radical. Hori et al.[3] concluded that the hydrogen abstraction by the mobile peroxy radical, $ROO\cdot + R'H \rightarrow ROOH + R'$, is not intramolecular but intermolecular. In this section, we will support their conclusion from the following experimental facts obtained in the present study. (1) It was confirmed that the motion of the unstable and mobile peroxy radicals was a rotation or rotatory vibration

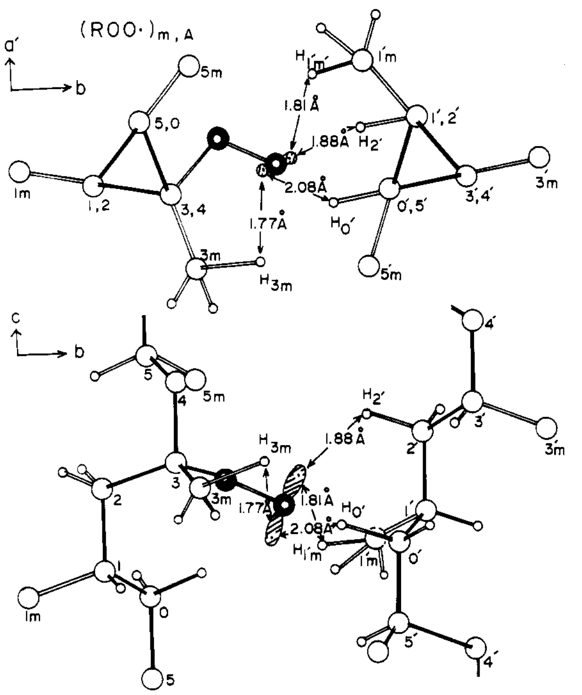

Figure 9. Model of a peroxy radical $(PO_1O_2\cdot)_{m,A}$ of isotactic polypropylene and its circumstances. The representative distances between the P_π orbital on oxygen atom, O_2 and hydrogen atoms are also shown. The large open circles and the small open circle indicate carbon and hydrogen atoms, respectively. The circles darkened on the exterior indicate oxygen atoms. The meanings of m and A of $(POO\cdot)_{m,A}$ are described in the text.

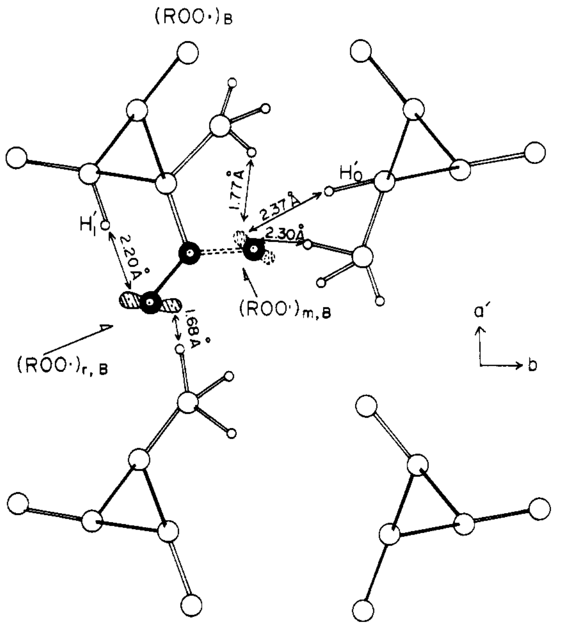

Figure 10. Model of peroxy radicals, $(POO\cdot)_{r,B}$ and $(POO\cdot)_{m,B}$ and their circumstance. Other interpretations for the figure are the same as for Figure 9. The meanings of r, m, and A of $(POO\cdot)_{r,A}$ and $(POO\cdot)_{m,B}$ are described in the text.

of the COO· group around the main chain axis, occurring also in the elongated sample. (2) The conformational structure of the mobile peroxy radicals is close to a skew conformation. (3) It can safely be concluded that the mobile peroxy radicals are trapped in the disordered sites in inner crystalline regions. In Figure 9 a model is given schematically for the hydrogen abstraction of the radical in *it*-polypropylene crystal (experimental fact (3)). In this model, we assume that the position of all carbon and hydrogen atoms remains unchanged when peroxy radical was formed. For instance, the 3_1 helical structure of *it*-polypropylene is preserved. Also, it was assumed that a half charge is located in each of two lobes of a oxygen P_π orbital and that the two half charges are separated by 1.34 Å. This value is calculated from the average distance of single and double O–O bonds for simplicity. We used the structure of *it*-polypropylene crystal reported by Natta et al.[16]

In Figure 9 we take an example of two nearest-neighbor main chains in the crystal. The same discussions can be expected for the other sets of two main chains. In Figure 9, the distances between a half charge and typical hydrogen atoms are shown in the case of the mobile peroxy radical. For the calculation, the conformational structure of the radical (ϕ_m = −103°) $(POO)_{m,A}$ was considered (experimental fact (2)). The distance between a half charge and a hydrogen in a methyl group was taken to be a minimum because of free rotation of the methyl group. Surprisingly, the distances between the half charge and the hydrogen atoms, H_{1m}', H_2' and H_0' of the interchain are the same order of magnitude in comparison with that in the case of the hydrogen atom, H_{3m}, of the intrachain and they are not widely different from the O–H bond distance, 0.96 Å. Therefore, the peroxy radical should abstract the intermolecular hyrogen H_{1m}', H_2', or H_0'. Hydrogen atoms, H_{1m}', H_2', and H_0' might be able to reach easily the P_π orbital of the peroxy radical by the rotation or the rotatory vibration of COO group, (Experimental fact (1)) but hydrogen atom, H_{3m} might not be able to reach it because of the small amplitude of intra-molecular vibrations. Another possibility for the structure can be considered. The peroxy radicals represented in Figure 10 (case (B)) are formed when oxygen molecules are attacked by the carbon radicals from the opposite side from the case of the peroxy radicals represented in Figure 9 (case (A)). The rigid radical in case (B) can be considered to be very stable because in $(ROO\cdot)_{r,B}$ the distances between the p-orbital and hydrogen atoms are the same order of magnitude in comparison with the radical in the case of (A) as represented in Figure 10 but the amplitude of the intra- and intermolecular vibration is small. On the other hand, the mobile radical in the case of (B), $(ROO\cdot)_{m,B}$, can abstract the interchain hydrogen atoms for the same reason as in the case of (A), $(ROO\cdot)_{m,A}$. The distance between a half charge and an intrachain hydrogen atom, H_{5m}, 1.00 Å in the case of (A) and gauche conformation (ϕ = 55.5°), $(ROO\cdot)_{r,A}$ is very close to the O–H bond distance, 0.96 Å. Therefore, the radical may abstract hydrogen atom H_{5m} as soon as the peroxy radical is formed. At the present stage, we cannot determine whether case (A) or case (B) is true.

However, it can be concluded that the mobile peroxy radicals should abstract the interchain hydrogen atoms. The reaction can be interpreted in terms of the conformational structure, the molecular motion, and the molecular disorder.

Acknowledgment. We express our thanks to Drs. S. Hibi and K. Kujita for their help in the analysis of the X-ray diffraction measurements. We are also grateful for A. Kotake's assistance in obtaining the data. Partial support of a Grant-in-Aid for Scientific Research from the Ministry of Education, Science and Culture of Japan is greatly acknowledged.

Registry No. Isotactic polypropylene (homopolymer), 25085-53-4.

References and Notes

(1) For example, (a) Shimada, S.; Tanigawa, T.; Kashiwabara, H. *Polymer* **1980**, *21*, 1176. (b) Shimada, S.; Hori, Y.; Kashiwabara, H. *Polymer* **1981**, *22*, 1377. (c) Hori, Y.; Shimada, S.;

Kashiwabara, H. *Polymer* **1977**, *18*, 1143. (d) Shimada, S.; Hori, Y.; Kotake, A.; Kashiwabara, H. *Macromolecules* **1984**, *17*, 1104.

(2) Eda, B.; Nunome, K.; Iwasaki, M. *J. Polym. Sci., Polym. Lett. Ed.* **1969**, *7*, 91.

(3) Hori, Y.; Shimada, S.; Kashiwabara, H. *J. Polym. Sci., Polym. Phys. Ed.* **1984**, *22*, 1407.

(4) Samuels, R. J. "Structured Polymer Properties"; Wiley: New York, 1974; Chapter 2, p 16.

(5) Shimada, S.; Williams, F. *Macromolecules* **1980**, *13*, 1721.

(6) Wilchinsky, W. *J. Appl. Phys.* **1959**, *30*, 792.

(7) Wilchinsky, W. *J. Appl. Polym. Sci.* **1963**, *1*, 923.

(8) Takahara, H.; Kawai, H.; Yamada, T. *Sen-i Gakkaishi* **1967**, *23*, 102.

(9) For example, James et al.[9a] assumed a Gaussian distribution, $C \exp(a \sin^2 \alpha + b \sin^4 \alpha)$. Others[9a-d] have used different distribution functions. (a) James, P. G.; Luckhurst, R. *Mol. Phys.* **1970**, *19*, 489. (b) Libertini, L. J.; Burle, P. C.; Jost, P. C.; Griffith, H. *J. Magn. Reson.* **1974**, *15*, 460. (c) Blum, H.; Salerno, C.; Leigh, J. S., Jr. *J. Magn. Reson.* **1978**, *30*, 385. (d) Swartz, J. C.; Hoffman, B. M.; Krizek, R. J.; Atmatzidis, D. K. *J. Magn. Reson.* **1979**, *36*, 259.

(10) Hori, Y.; Makino, Y.; Kashiwabara, H. *Polymer* **1984**, *25*, 1436.

(11) Iwasaki, M.; Sakai, Y. *J. Polym. Sci., Part A-2* **1968**, *6*, 265.

(12) Hori, Y.; Aoyama, S.; Kashiwabara, H. *J. Chem. Phys.* **1981**, *75*, 1582.

(13) Kusumoto, N.; Matsumoto, K.; Takayanagi, M. *J. Polym. Sci., Part A-1* **1969**, *7*, 1173.

(14) (a) Fisher, H.; Hellwege, K. H.; Newdörfl, P. *J. Polym. Sci.*, Part *A* **1963**, *1*, 2109. (b) Fisher, H.; Hellwege, K. H.; Johnson, U.; Newdörfl, P. *Kolloid-Z* **1964**, *195*, 129.

(15) (a) Nunome, K.; Eda, B.; Iwasaki, M. *J. Polym. Sci., Part A-1* **1970**, *8*, 1831. (b) Nunome, K.; Eda, B.; Iwasaki, M. *J. Appl. Polym. Sci.* **1974**, *18*, 2711. (c) Nunome, K.; Eda, B.; Iwasaki, M. *J. Appl. Polym. Sci.* **1974**, *18*, 2719.

(16) Natta, G.; Corradini, P. *Nuovo Ciment, Suppl.* **1960**, *15*, 40.

The Involvement of Stilbene in Radical Polymerizations of Methyl Methacrylate and Styrene

John C. Bevington* and Thomas N. Huckerby

Department of Chemistry, The University, Lancaster, U.K. *Received June 25, 1984*

ABSTRACT: Polymerizations of methyl methacrylate and styrene, initiated by benzoyl-*carbonyl*-^{13}C peroxide and performed in the presence of *trans*-stilbene, lead to polymers containing appreciable numbers of the end groups $C_6H_5COOCH(C_6H_5)CH(C_6H_5)-$ detected by NMR spectroscopy; very little stilbene is incorporated in the polymer chains. When the polymerizations are initiated by sources of the radical $(^{13}CH_3)_2C(CN)\cdot$, there is negligible reaction of the primary radicals with stilbene. The results show that stilbene is very reactive toward the oxygen-centered benzoyloxy radical but very unreactive toward the carbon-centered 2-cyano-2-propyl, poly(methyl methacrylate), and polystyrene radicals.

This paper is concerned mainly with the effects of *trans*-stilbene (STL) upon initiation processes in the radical polymerizations of methyl methacrylate (MMA) and styrene (STY) using benzoyl peroxide (BPO), azoisobutyronitrile (AIBN), and 2-cyano-2-propylazoformamide (AZOF). It provides another example of the applications of NMR spectroscopy to studies of end groups and the value of the procedure for the understanding of the reactions occurring in polymerizing systems.

The rate of decomposition of BPO in benzene at 60 °C is unaffected by the presence of STL at concentrations up to at least 50 g/L but there are marked reductions in the yield of carbon dioxide formed by decarboxylation of benzoyloxy radicals.[1] The presence of STL causes only slight increases in the amount of benzoic acid produced in the systems and so the effects on the production of carbon dioxide can be explained by ascribing to the additive high reactivity for capture of $C_6H_5COO\cdot$ radicals. This conclusion has been confirmed by results of experiments in which BPO was used to initiate polymerizations of STY and MMA in the presence of STL.[2] The rate of polymerization was not affected by the presence of the additive but the balance between benzoate and phenyl end groups in the polymers was shifted, in the sense that the proportion of the ester end groups was increased. it appeared that the polymers contained comparatively high proportions of the end groups $C_6H_5COOCH(C_6H_5)CH(C_6H_5)-$.

The results indicate that the reactivities at 60 °C of STY, MMA, and STL for capturing the benzoyloxy radical are in the proportions 1.0:0.12:4.8. The high reactivity of STL toward the radical $C_6H_5COO\cdot$ can be contrasted with its low reactivity toward polymer radicals of various types as shown by its failure to copolymerize with STY[3] or MMA.[2]

To study further the reactions of STL with primary radicals, use has been made of a new procedure for examination of the reactivities of unsaturated substances.[4] Radicals enriched with carbon-13 are generated in a mixture of monomers. From the NMR spectrum of the resulting copolymer, it is possible in suitable cases to compare the numbers of primary radicals attached to the two types of monomer unit and then to find the relative values of the velocity constants for the reactions of the radical with the two monomers. In the present work, benzoyl-*carbonyl*-^{13}C peroxide (^{13}C-BPO) has been used as a source of $C_6H_5{}^{13}COO\cdot$ radicals at 60 °C; $(^{13}CH_3)_2C(CN)\cdot$ radicals have been generated from suitably enriched AIBN at 60 °C or AZOF at 100 °C.

Experimental Section

Details have already been given of preparations and purifications of materials and of procedures for recording ^{13}C NMR spectra using a JEOL FX100 Fourier-transform spectrometer operating at 25.05 MHZ.[2,4,5] Polymerizations were performed with toluene as diluent in sealed tubes in the absence of air; conversions did not exceed 10%. Polymers were recovered by precipitation in methanol, purified by reprecipitation, and dried in vacuum at 50 °C; tests showed that complete removal of unreacted initiator and monomers was achieved.

Results and Discussion

Polymers of MMA were prepared at 60 °C by using monomer at about 2 mol/L, ^{13}C-BPO at about 2 g/L, and various concentrations of STL so that the values of

0024-9297/85/2218-0176$01.50/0